Journal of New Materials for Electrochemical Systems 12, 207-212 (2009)

Electrochemical Performance of $SnPO_4$-coated $LiNi_{1/3}Mn_{1/3}Co_{1/3}O_2$ Cathode Materials

Hyun-Soo Kim[*,1], Woo-Seong Kim[2], Hal-Bon Gu[3] and Guoxiu Wang[4]

[1]Battery Research Center, Korea Electrotechnology Research Institute, Changwon 641-120, Korea
[2]Daejung EM Co., Incheon 405-820, Korea
[3]Dept. of Electrical Eng., Chonnam National University, Gwangju 500-757, Korea
[4]School of Mechanical, Materials and Mechatronic Engineering, University of Wollongong, NSW 2522, Australia

Received: September 15, 2009, Accepted: September 25, 2009

Abstract: *A Sn phosphate was successfully coated to the surface of $LiNi_{1/3}Co_{1/3}Mn_{1/3}O_2$ particles using a new method we developed. The elements Sn and P were observed to be uniformly distributed on the surface of the $LiNi_{1/3}Co_{1/3}Mn_{1/3}O_2$. After the Sn phosphate coating, the onset temperature shifted up to about 250 °C, and the exothermic value also decreased to 116.3 J/g, i.e. the thermal stability of the material was enhanced.*

The rate capability of the 1 wt% Sn phosphate-coated $LiNi_{1/3}Co_{1/3}Mn_{1/3}O_2$ materials was enhanced at room temperature and 60 °C. However, a 3 wt% Sn phosphate coating degraded the electrochemical performance. The 1 wt% Sn phosphate-coated material showed improved cycle performance compared to that of the bare material at room temperature and 60 °C. It is believed that the oxide coating layer prevented direct contact with the organic electrolyte.

Keywords: $SnPO_4$, $LiNi_{1/3}Mn_{1/3}Co_{1/3}O$, thermal stability, rate capability, cycle performance

1. INTRODUCTION

$LiCoO_2$ has been widely used as a cathode material in commercial Li-ion batteries because of its excellent electrochemical properties and the ease of preparation [1,2]. However, the practical specific capacity of $LiCoO_2$ is limited to below 140 mAh·g^{-1} on charging up to 4.2 V vs. Li ($Li_{0.5}CoO_2$), even though its theoretical capacity is 274 mAh·g^{-1}. Furthermore, it is expensive and has relatively low thermal stability [3]. To overcome these drawbacks of $LiCoO_2$ cathode material, which limits its use in high volumetric energy density batteries, new cathode materials such as $LiNi_{0.8}Co_{0.2}O_2$ [4], $LiNi_{0.5}Co_{0.5}O_2$ [5], $LiNi_{0.5}Mn_{1.5}O_4$ [6], and $LiNi_xCo_{1-2x}Mn_xO_2$ [7] have been synthesized by substituting electrochemically-active metals, such as Ni and Mn, at the Co-site in $LiCoO_2$. Among these, $LiNi_{1/3}Co_{1/3}Mn_{1/3}O_2$ has attracted significant attention as a promising cathode material, due to its many advantages over $LiCoO_2$, such as high capacity, structural and thermal stability, and excellent cyclic performance [8-12].

We have previously shown that electrochemically-inactive metals such as Mg, Nb, Si, and Zr can be doped into the $LiNi_{1/3}Co_{1/3}Mn_{1/3}O_2$ matrix to further enhance its electrochemical properties and thermal stability [13]. Moreover, for similar reasons, the surface coating of $LiNi_{1/3}Co_{1/3}Mn_{1/3}O_2$ with Al_2O_3 and $LiAlO_2$ has been attempted using a sol-gel method [14,15], and excellent capacity retention was observed at charge cut-off voltages over 4.2 V.

This work has focused on the preparation and electrochemical properties of $SnPO_4$-coated $LiNi_{1/3}Co_{1/3}Mn_{1/3}O_2$. The surface coating of $LiNi_{1/3}Co_{1/3}Mn_{1/3}O_2$ with $SnPO_4$ has been tried for the first time to improve its electrochemical properties. The effects of the $SnPO_4$ coating on $LiNi_{1/3}Co_{1/3}Mn_{1/3}O_2$ were examined with respect to rate capability, cycle life, impedance spectroscopy and differential scanning calorimetry (DSC) measurements.

2. EXPERIMENTAL

$Ni_{1/3}Co_{1/3}Mn_{1/3}(OH)_2$ starting powders were prepared by a co-precipitation from a solution containing stoichiometric amounts of nickel sulfate ($NiSO_4·6H_2O$), cobalt sulfate ($CoSO_4·7H_2O$), and manganese sulfate ($MnSO_4·5H_2O$) by the addition of NaOH and NH_4OH solutions. The pH was maintained between 11 and 12 by

*To whom correspondence should be addressed: Email: hskim@keri.re.kr
Phone: +82-55-280-1663, Fax : +82-55-280-1590

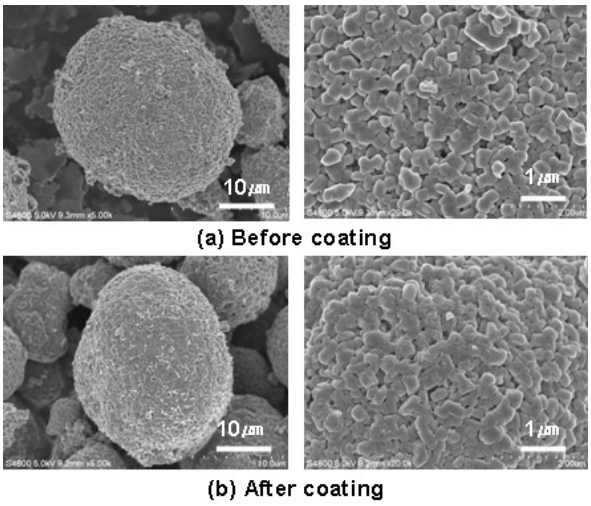

Figure 1. SEM morphologies of the bare- and $SnPO_4$-coated $LiNi_{1/3}Mn_{1/3}Co_{1/3}O_2$ cathode materials.

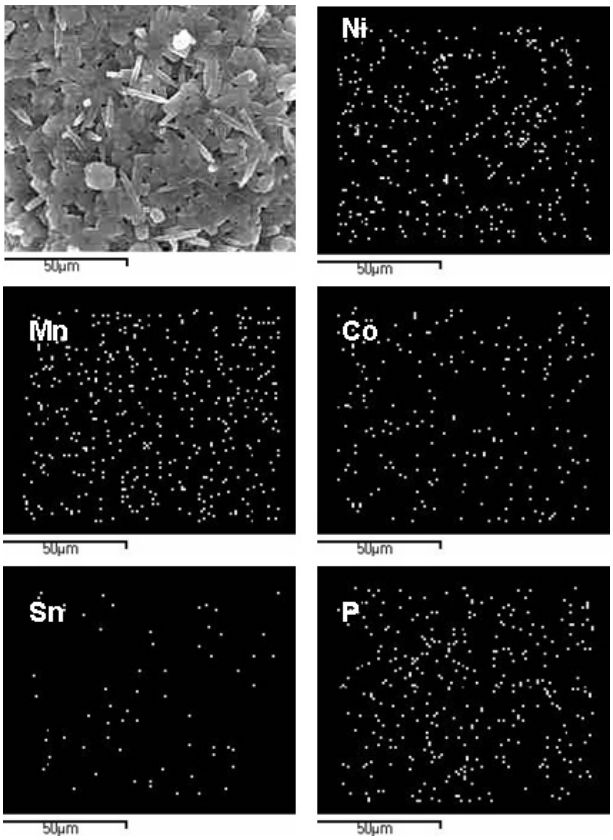

Figure 2. EDS profiles of $SnPO_4$-coated $LiNi_{1/3}Mn_{1/3}Co_{1/3}O_2$ cathode materials.

controlling the amount of NaOH. The particle size was controlled by the pH, reaction time, and stirring speed. Spherical particles (~10 μm diameter) were uniformly produced under the conditions of pH 11, reaction time 12 h, and 1,000 rpm. To prepare $LiNi_{1/3}Co_{1/3}Mn_{1/3}O_2$ powders, stoichiometric amounts of the as-prepared $Ni_{1/3}Co_{1/3}Mn_{1/3}(OH)_2$ and $LiOH{\cdot}H_2O$ were mixed, calcined, and then sintered at 1000 ºC for 10h. For an 1 wt% $SnPO_4$ coating on 10 g of $LiNi_{1/3}Co_{1/3}Mn_{1/3}O_2$ powders, 0.411 g of Sn-acetate and 0.130 g of $NH_4H_2PO_4$ were dissolved in distilled water and stirred for 1 h at 20 ºC, and then $LiNi_{1/3}Co_{1/3}Mn_{1/3}O_2$ powders were slowly added and thoroughly mixed for 20 min. After filtering, the mixture was dried at 120 ºC for 12 h.

Scanning electron microscope (SEM) images of the bare and $SnPO_4$-coated $LiNi_{1/3}Co_{1/3}Mn_{1/3}O_2$ were obtained using a Hitachi S-4800 machine. Differential scanning calorimetry (DSC) experiments were conducted on the bare and $SnPO_4$-coated $LiNi_{1/3}Co_{1/3}Mn_{1/3}O_2$ samples charged to 4.3 V (vs. metallic Li). The data were acquired using a TA Instrument Q1000 differential scanning calorimeter at a scan rate of 10 ^oC/min in the temperature range of 50-350 ^oC.

The electrodes were fabricated from an 86: 8: 6 (mass%) mixture of active material: polyvinylidene difluoride (PVDF, Aldrich) as binder: Super-P carbon black (MMM Carbon) as current conductor. The PVDF was dissolved in N-methylpyrrolidinone (NMP, Kanto), and the active material and conductor mixture were added. After homogenization, the slurry was evacuated for 20 min to remove the residual air. The slurry was then coated onto thin aluminum foil (14 μm thick) and dried overnight at 110 ºC. The electrode was pressed with a pressure of 600 to 800 $kg{\cdot}cm^{-2}$ and punched into 15 mm diameter disks.

The electrochemical cells were prepared in standard 2032 coin cell hardware with lithium metal foil used as both the counter and reference electrodes. Cells were assembled in a dry room (dew point below -55 ºC). The electrolyte used for analysis was 1.0 M $LiPF_6$ in ethylene carbonate/ diethyl carbonate (EC/DEC, 1/1). The cells were taken out of the dry room and placed on the battery testing system (TOSCAT 3100). The cells were aged for 5 h before the first charge to ensure full absorption of the electrolyte into the electrode.

To evaluate the rate capabilities, various current rates such as the 0.2C, 0.5C, 1C, 2C, and 5C rates were used at room temperature and 60 ^oC. The charge and discharge cycling tests of the cells were conducted galvanostatically at the 1C rate over a voltage range of 4.3 to 2.8 V at room temperature and 60 ^oC. The electrochemical impedance spectroscopy (EIS) results on the obtained cell were evaluated using an AC impedance analyzer after charge and discharge cycling. AC impedance measurements were performed by using a Zahner Elektrik IM6 impedance analyzer over a frequency range of 700 mHz to 2 MHz for interface investigation of the cells.

3. RESULTS AND DISCUSSION

Fig. 1 shows SEM images of the bare- and stannum phosphate-coated powder. The primary particles with a particle size of 400 nm were aggregated and formed spherical secondary particles about 12 μm in diameter. In the SEM image for the Sn phosphate-coated powders, the stannum phosphate was coated uniformly on the surface of the secondary particles. This confirms that the stannum phosphate coating was applied successfully using with our new coating method.

Fig. 2 shows energy dispersive spectroscopy (EDS) images of

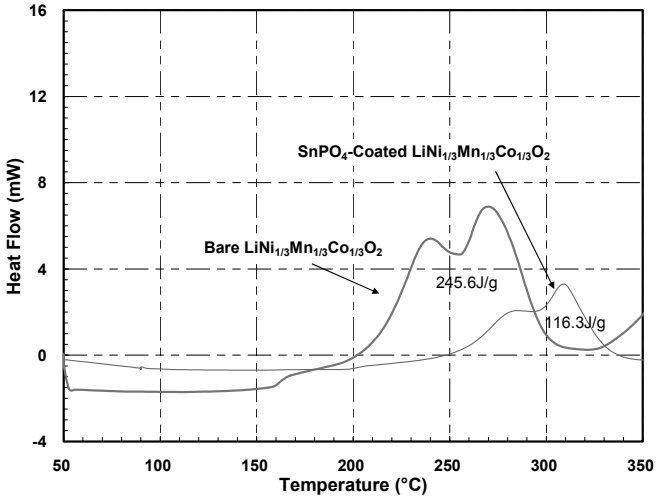

Figure 3. DSC profiles of the bare- and $SnPO_4$-coated $LiNi_{1/3}Mn_{1/3}Co_{1/3}O_2$ cathode materials.

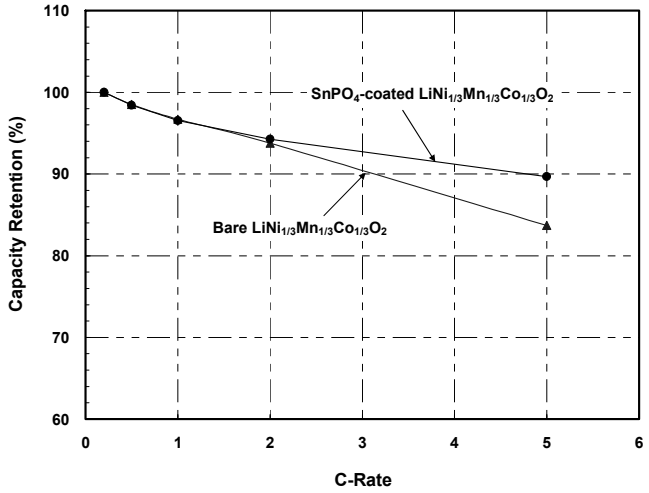

Figure 5. Capacity retention of the bare- and $SnPO_4$-coated $LiNi_{1/3}Mn_{1/3}Co_{1/3}O_2$ cathode materials at various different current rates at 60 ^oC.

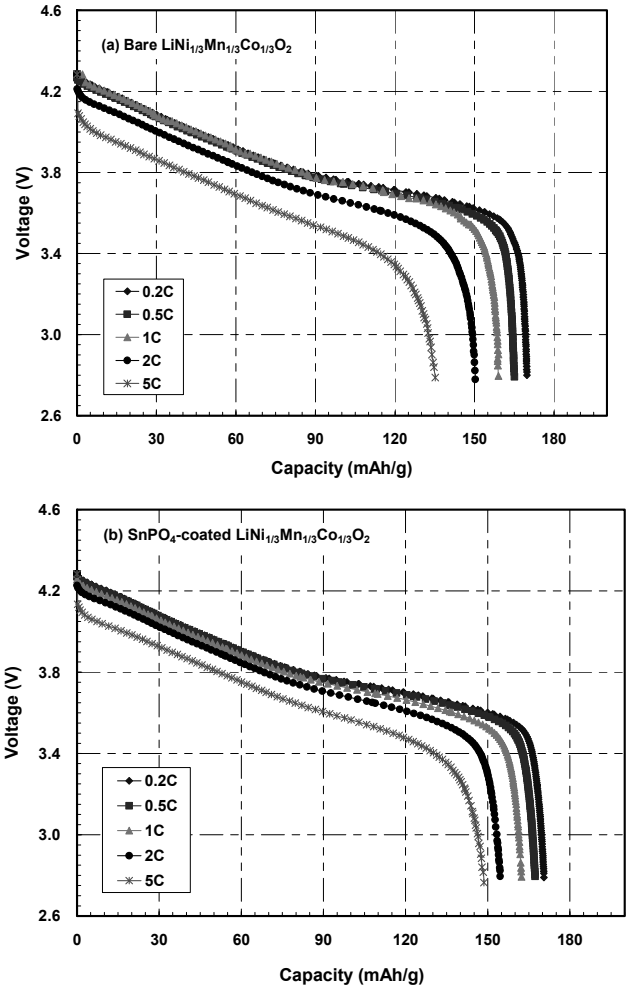

Figure 4. Rate capability of the bare- and $SnPO_4$-Coated $LiNi_{1/3}Mn_{1/3}Co_{1/3}O_2$ Cathode Materials at room temperature.

the stannum phosphate-coated powder to measure the chemical components on the surface of the materials. As seen as in the figure, the elements Sn and P were detected on the surface of a secondary particle in a 20,000 × enlarged image.

Fig. 3 shows the DSC profiles of the bare- and Sn phosphate-coated powders that were obtained to evaluate the thermal stability of the materials. Measurements were taken after full charging to 4.3 V. As seen as in the figure, the peak volume and position of an exothermic reaction, which implies oxygen decomposition in the active material, were changed after the Sn phosphate coating was applied. In the bare material, the onset temperature, at which the temperature increases in the initial stage, and the caloric value were about 200 ^oC and 245.6 J/g, respectively. However, with the Sn phosphate coating, the onset temperature shifted up to about 250 ^oC and the exothermic value also decreased to 116.3 J/g. Therefore we can suggest that the Sn phosphate coating enhances the thermal stability of the $LiNi_{1/3}Co_{1/3}Mn_{1/3}O_2$ powder material. There are several reports that an oxide coating on the surface of the active material can improve its thermal stability [16-21].

Fig. 4 show the charge/discharge curves of $Li/LiNi_{1/3}Co_{1/3}Mn_{1/3}O_2$ cells at various current rates (0.2C - 5C) at room temperature. The samples were charged using a current rate of 0.2C and discharged with the given current rate. Fig. 4(a) shows the rate capability of the bare material, which delivered a discharge capacity of 169.8 mAh/g at the 0.2C rate, with the discharge capacity slowly decreasing with increasing current rate. The discharge capacity decreased to 135.2 mAh/g at a 5C rate: capacity retention was 79.6 % compared with the 0.2C rate. However, the Sn-phosphate coated material gave a discharge capacity of 170.6 mAh/g at the 0.2C rate. The discharge capacity of the coated material was 148.6 mAh/g at the 5C rate: capacity retention was 87.1% compared with the 0.2C rate. Namely, the rate capability of the coated electrode was also enhanced.

Fig. 5 show the charge/discharge curves of $Li/LiNi_{1/3}Co_{1/3}Mn_{1/3}O_2$ cells at various current rates (0.2C - 5C) at

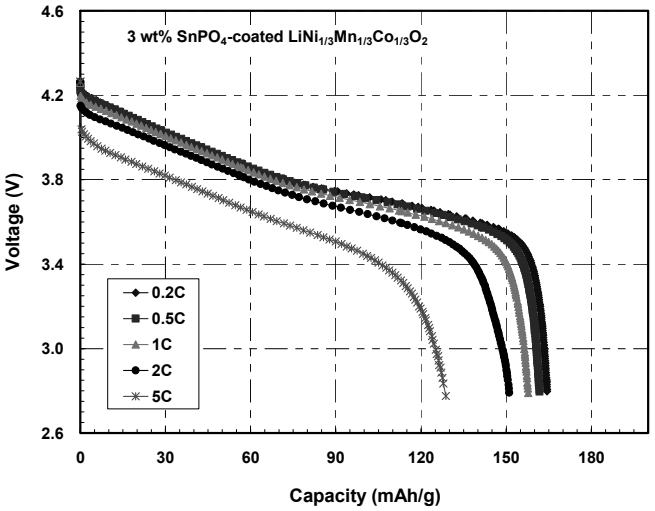

Figure 6. Rate capability of 3 wt% $SnPO_4$-coated $LiNi_{1/3}Mn_{1/3}Co_{1/3}O_2$ cathode materials at room temperature.

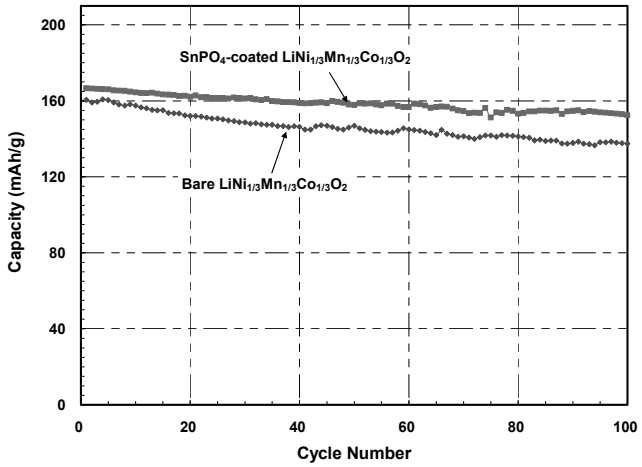

Figure 7. Cycle performances of the bare- and $SnPO_4$-coated $LiNi_{1/3}Mn_{1/3}Co_{1/3}O_2$ cathode materials at 1C rate at room temperature.

60 °C. The rate capability of the Sn phosphate coated material was enhanced at elevated temperature as well as the initial discharge capacity. The discharge capacity of the bare material was 182.3 mAh/g at the 0.2C rate, although it delivered a capacity of 169.8 mAh/g at room temperature. The discharge capacity decreased to 152.6 mAh/g at the 5C rate: capacity retention was 83.7 % compared with the 0.2C rate. However, the Sn-phosphate coated material delivered a discharge capacity of 180.4 mAh/g at the 0.2C rate. The discharge capacity of the coated electrode was 161.8 mAh/g at the 5C rate: capacity retention was 89.7 % compared with the 0.2C rate. In fact, the rate capability of the coated electrode was even enhanced at 60 °C. The reason for the enhanced rate capability was that the Sn-phosphate coating reduces the interface resistance between the active material and the electrolyte.

Fig. 6 shows the voltage profiles of the 3 wt% Sn phosphate-

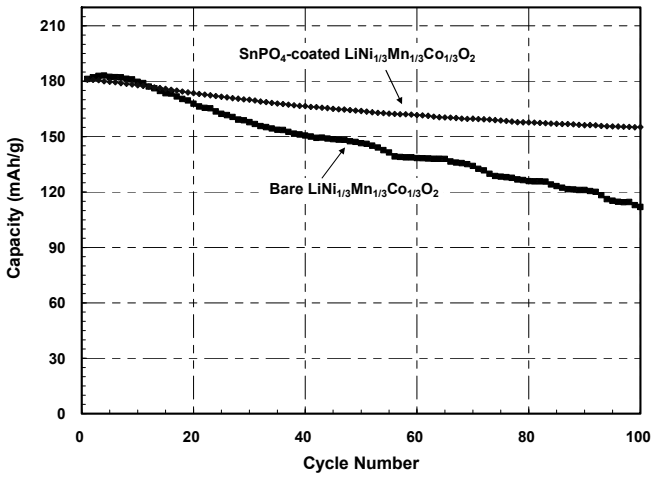

Figure 8. Cycle performances of the bare- and $SnPO_4$-coated $LiNi_{1/3}Mn_{1/3}Co_{1/3}O_2$ cathode materials at 1C rate at a temperature of 60 °C.

coated powder that were obtained at various current rates. As seen in the figure, the initial capacity decreased to 164.5 mAh/g, and the rate performance was also degraded compared with the bare material. The discharge capacity was 128.8 mAh/g at the 5C rate, and the capacity retention were 78.3 % compared with the 0.2C rate. It is assumed that a 3 wt% Sn phosphate coating provides a thicker barrier to Li^+ ion transport at the surface of the $Li/LiNi_{1/3}Co_{1/3}Mn_{1/3}O_2$, so that electronic and ionic conduction among the particles becomes limited.

Fig. 7 shows the cycle performance of the Sn phosphate-coated material at the 1C current rate in the voltage range of 4.3-2.8V. The initial discharge capacity of the non-coated powder was measured to be 160.1 mAh/g, and it decreased with cycling, having a retained capacity of 137.5 mAh/g: 85.9 % retention capacity after 100 cycles. Nevertheless, the initial discharge capacity of the coated electrode measured 166.3 mAh/g and then remained at 152.4 mAh/g, with 91.7% of capacity retained after 100 cycles. The retention capacity was increased by exactly 5.8 % as a result of the Sn-phosphate coating. It is believed that the oxide coating layer prevents direct contact with an organic electrolyte. The cycle-life performances of bare and 3 wt% Sn-phosphate-coated $LiNi_{1/3}Co_{1/3}Mn_{1/3}O_2$, at the 1C rate between 4.3 and 2.8 V at the temperature of 60 °C, are presented in Fig. 8. The initial discharge capacity (182.3 mAh/g) of the bare $LiNi_{1/3}Co_{1/3}Mn_{1/3}O_2$ decreased gradually with cycling; it finally reached 111.9 mAh/g after 100 cycles, i.e., 61.4 % of its initial discharge capacity. The capacity retention at 60 °C was higher than at room temperature. The 1 wt% Sn phosphate-coated $LiNi_{1/3}Co_{1/3}Mn_{1/3}O_2$ exhibited enhanced capacity retention upon cycling at elevated temperature.

Electrochemical impedance spectroscopy (EIS) was performed to gain understanding of the cycle-life and rate capability characteristics of the bare and Sn phosphate-coated $LiNi_{1/3}Co_{1/3}Mn_{1/3}O_2$ cathode materials. Similar EIS studies have also been reported for many other cathode materials, such as $LiCoO_2$ [22], $Li(Ni_{0.8}Co_{0.2})O_2$ [23,24], TiO_2-coated $Li(Ni_{0.8}Co_{0.2})O_2$ [24], and $AlPO_4$-coated $Li(Ni_{0.8}Co_{0.2})O_2$ [19]. Fig. 9 shows the EIS

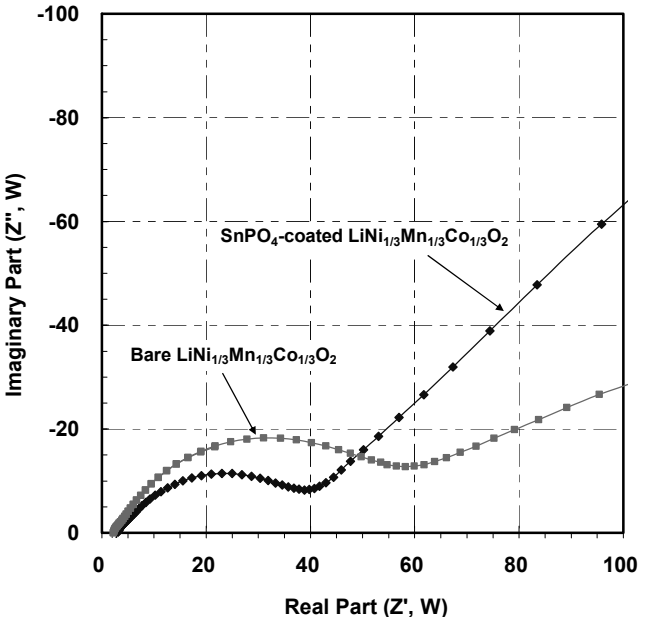

Figure 9. Impedance spectra of the bare- and $SnPO_4$-coated $LiNi_{1/3}Mn_{1/3}Co_{1/3}O_2$ cathode materials at a temperature of 60 ^oC.

of the bare and Sn phosphate-coated $LiNi_{1/3}Co_{1/3}Mn_{1/3}O_2$, respectively, after 50 cycles between 4.3 and 2.8V at the 1C rate. As seen in Fig. 9, the surface film resistance component of the sample decreases after the Sn phosphate coating has been applied on the surface of the $LiNi_{1/3}Co_{1/3}Mn_{1/3}O_2$ powder. Two semicircles were clearly observed on the Bode graph when the samples were scanned down to a frequency of 1 mHz.

In general, The semicircle in the high frequency range was related to the Li-ion migration resistance (R_f) through the surface film formed on the cathode surface. The intermediate frequency semicircle is attributed to the charge transfer process (resistance) in the cathode/electrolyte interface [24-26]. Significantly, the high-frequency semicircle of the coated phase is much smaller than that of the bare phase. Since the corrosion or dissolution of the cathode material in a liquid electrolyte generally leads to the formation of resistive reaction layers on the surface of the cathode materials during the charging and discharging processes, in this case, the high frequency semicircle of the bare electrode can be attributed to the resistive reaction layer. The smaller high-frequency semicircle observed in the impedance spectra of the Sn phosphate-coated phase indicates that the reaction between the cathode and the electrolyte is suppressed by the Sn phosphate coating. The coating layer seems to protect the $LiNi_{1/3}Co_{1/3}Mn_{1/3}O_2$ particles from dissolution in the electrolyte. This leads to the improvement in the cycle-life of the stannum phosphate-coated $LiNi_{1/3}Co_{1/3}Mn_{1/3}O_2$, because the coating reduces the contact area of the charged active material with the electrolyte. Similar results were also observed in many other coated cathode materials, such as Al_2O_3- and ZrO_2-coated $LiCoO_2$ [27,28] and $AlPO_4$- and TiO_2-coated Li $Ni_{0.8}Co_{0.2}O_2$ [19,24]. In addition to preventing the dissolution of the cathode materials in liquid electrolyte, the coating layer was reported to dramatically reduce the crystallographic deformation of the cathode materials during charge and discharge [19,27,29].

Hence, the enhanced cycle-life in the stannum phosphate-coated $LiNi_{1/3}Co_{1/3}Mn_{1/3}O_2$ is expected to be a complex phenomenon which is related to both the cathode/electrolyte interface stability and the stabilized structure of the cathode. This latter feature is also thought to be behind the improved rate capability of the $LiNi_{1/3}Co_{1/3}Mn_{1/3}O_2$ cathode that occurs after Sn phosphate coating. Since the major cause of decrease in the rate capability has been reported to be the strains and defects generated by fast Li^+ extraction and intercalation in the cathode material [19,27,29], it is proposed that the coating layer reduces the the strains and defects in the particles by stabilizing the layered structure of the $LiNi_{1/3}Co_{1/3}Mn_{1/3}O_2$.

4. CONCLUSIONS

A Sn phosphate coating was successfully applied on the surface of $LiNi_{1/3}Co_{1/3}Mn_{1/3}O_2$ particles using our new coating method. The elements Sn and P were observed to be distributed uniformly on the surface of the $LiNi_{1/3}Co_{1/3}Mn_{1/3}O_2$ by EDS. After the Sn phosphate coating, the onset temperature shifted up to about 250 ^oC, and the exothermic value also decreased to 116.3 J/g, i.e. the thermal stability of the material was enhanced.

The rate capability of the 1 wt% Sn phosphate-coated $LiNi_{1/3}Co_{1/3}Mn_{1/3}O_2$ materials was enhanced. The Sn phosphate-coated electrode showed 87.1% capacity retention, compared with 79.6% before coating. However, the 3 wt% Sn phosphate coating provided a thicker barrier to Li^+ ion transport at the surface of the $Li/LiNi_{1/3}Co_{1/3}Mn_{1/3}O_2$, so that the rate capability became degraded. The Sn phosphate-coated electrode showed improved cycling performance compared to that of the bare electrode at room temperature and 60 ^oC. The initial discharge capacity of the coated electrode measured 166.3 mAh/g and then remained at 152.4 mAh/g, 91.7% capacity retention, after 100 cycles. It is believed that the oxide coating layer prevents direct contact with the organic electrolyte.

5. ACKNOWLEDGMENTS

This research was supported by a grant (code number: 08K1501-01510) from the Center for Nanostructured Materials Technology under the 21st Century Frontier R&D Programs of the Ministry of Education, Science and Technology, Korea.

REFERENCES

[1] J. N. Reimers, J. R. Dahn, J. Electrochem. Soc., 139, 2091 (1992).
[2] T. Ohzuku, A. Ueda, J. Electrochem. Soc., 141, 2972 (1994).
[3] J. Kim, C. Park, Y. Sun, Solid State Ionics, 164, 43 (2003).
[4] S. Wu, C.W. Yang, J. Power Sources, 146, 270 (2005).
[5] I. Belharouak, H. Tsukamoto, K. Amine, J. Power Sources, 119-121, 175 (2003).
[6] Y. Talyosef, B. Markovsky, G. Salitra, D. Aurbach, H. Kim, and S. Choi, J. Power Sources, 146, 664 (2005).
[7] D. D. MacNeil, Z. H. Lu, J. R. Dahn, J. Electrochem. Soc., 149, A1332 (2002).
[8] K. M. Shaju, G. V. S. Rao, B. V. R. Chowdari, Electrochim. Acta, 48, 145 (2002).

[9] N. Yabuuchi, T. Ohzuku, J. Power Sources, 119, 171 (2003).
[10]D.-C. Li, T. Muta, Li.-Qi. Zhang, M. Yoshio, H. Noguchi, J. Power Sources, 132, 150 (2004).
[11]H. Y. Xu, S. Xie, C. P. Zhang, C. H. Chen, J. Power Sources, 148, 90 (2005).
[12]T. Ohzuku, Y. Makimura, Chem. Lett., 7, 642 (2001).
[13]S. Na, H. Kim, and S. Moon, Solid State Ionics, 176, 313 (2005).
[14]Y. Kim, H. Kim, and S. W. Martin, Electrochimica Acta, 52, 1316 (2006).
[15]H. Kim, Y. Kim, S. Kim, and S. W. Martin, J. Power Sources, 161, 623 (2006).
[16]J. Cho, Y. W. Kim, B. Kim, B. Park, Angew. Chem. Int. Ed., 42, 16181 (2003).
[17]J. Kim, M. Noh, J. Cho, H. Kim, K. Kim, J. Electrochem. Soc., 152, A1142 (2005).
[18]S. Oh, J. K. Lee, D. Byun, W. I. Cho, B. W. Cho, J. Power Sources, 132, 249 (2004).
[19]K. S. Tan, M. V. Reddy, G. V. Subba Rao, B. V. R. Chowdari, J. Power Sources, 141, 129 (2005).
[20]J. Cho, T.-J. Kim, J. Kim, M. Noh, B. Park, J. Electrochem. Soc., 151, A1899 (2004).
[21]A. Bibby, L. Mercier, Chem. Mater., 14, 1594 (2002).
[22]Y. M. Choi, S. I. Pyun, Solid State Ionics, 99, 173 (1997).
[23]F. Nobili, F. Croce, B. Scrosati, R. Marassi, Chem. Mater., 13, 1642 (2001).
[24]Z. R. Zhang, H. S. Liu, Z. L. Gong, Y. Yang, J. Power Sources, 129, 101 (2004).
[25]M. D. Levi, G. Salitra, B. Markovsky, H. Teller, D. Aurbach, U. Heider, L. Heider, J. Electrochem. Soc., 146, 1279 (1999).
[26]K. A. Striebel, E. Sakai, E. J. Cairns, J. Electrochem. Soc., 149, A61 (2002).
[27]J. Cho, Y. J. Kim, T. J. Kim, B. Park, Angew. Chem. Int. Ed., 40, 3367 (2001).
[28]Z. Chen, J. R. Dahn, Electrochem. Solid-State Lett., 5, 213 (2002).
[29]J. Cho, Y. J. Kim, B. Park, Chem. Mater., 12, 3788 (2000).